An analysis of the explosion limits of hydrogen–oxygen mixtures

ARTICLE *in* THE JOURNAL OF CHEMICAL PHYSICS · APRIL 2013

Impact Factor: 2.95 · DOI: 10.1063/1.4798459 · Source: PubMed

An analysis of the explosion limits of hydrogen-oxygen mixtures

Xianming Wang and Chung K. Law

Citation: J. Chem. Phys. **138**, 134305 (2013); doi: 10.1063/1.4798459
View online: http://dx.doi.org/10.1063/1.4798459
View Table of Contents: http://jcp.aip.org/resource/1/JCPSA6/v138/i13
Published by the American Institute of Physics.

An analysis of the explosion limits of hydrogen-oxygen mixtures

Xianming Wang (王贤明)[1] and Chung K. Law[1,2,a)]
[1]*Center for Combustion Energy and Department of Thermal Engineering, Tsinghua University, Beijing 100084, China*
[2]*Department of Mechanical and Aerospace Engineering, Princeton University, Princeton, New Jersey 08544-5263, USA*

(Received 26 December 2012; accepted 12 March 2013; published online 4 April 2013)

In this study, the essential factors governing the Z-shaped explosion limits of hydrogen-oxygen mixtures are studied using eigenvalue analysis. In particular, it is demonstrated that the wall destruction of H and HO_2 is essential for the occurrence of the first and third limits, while that of O, OH, and H_2O_2 play secondary, quantitative roles for such limits. By performing quasi-steady-state analysis, an approximate, cubic equation for the explosion limits is obtained, from which explicit expressions governing the various explosion limits including the state of the loss of non-monotonicity are derived and discussed. © *2013 American Institute of Physics*. [http://dx.doi.org/10.1063/1.4798459]

I. INTRODUCTION

Perhaps one of the most fascinating and practically important phenomena demonstrating the essential role of chain mechanisms in the discipline of chemistry is the non-monotonic explosion limits of hydrogen-oxygen mixtures.[1–3] Specifically, the explosion boundary of an H_2-O_2 mixture in a heated and pressurized chamber is typically Z-shaped in the temperature-pressure plane (see, e.g., Fig. 1(b)), consisting of two turning points that segment the transition boundary into the first, second, and third limits in the low, middle, and high pressure regimes, respectively. Consequently at moderate temperatures, the mixture is sequentially non-explosive, explosive, non-explosive, and explosive again as the pressure increases from a low value. It is obvious that such a behavior lies in the detailed chemistry which is more complex than can be described by the simple one-step overall reaction: $2H_2 + O_2 \rightarrow 2H_2O$. Furthermore, since the H_2-O_2 chemistry is an essential component of hydrocarbon oxidation, the underlying kinetic mechanism responsible for the non-monotonicity must necessarily permeate their oxidation mechanisms leading, for example, to recently observed non-monotonic response of the global kinetic parameters governing laminar flame propagation.[4]

Extensive studies (e.g., Refs. 1 and 2) have conclusively demonstrated that the nonmonotonic response is controlled by gas-phase chain branching reactions competing with gas-phase and surface termination reactions. Many of the prior studies were however primarily concerned with the second limit and processes associated with it because they are minimally affected by surface processes. In addition to the identification of the second limit in static environments, representative literature on the different topics of investigation include inhibition of the H-O_2 chain reactions through the addition of various hydrocarbons;[5,6] oscillatory ignition in continuous-flow, well-stirred reactors;[7–9] development of model chain-thermal theories of ignition;[10] and second-limit effects on shock-induced ignition.[11–14] While these worthwhile studies are not directly related to the central theme expounded in the present investigation, the richness of the phenomena and the potential extension of the understanding gained herein to the auxiliary processes are noted with interest.

Regarding the complete Z-curve response of the three explosion limits, and the essential role of surface termination in effecting the first and third limits, there is considerable uncertainty in the relative efficiencies for the destruction of the chain-carrying intermediates. For example, Semenov[1] obtained the first limit and found that H destruction is quantitatively more important than O and OH destruction, while Glassman and Yetter[3] stated that OH destruction may play a similar, crucial role as that of H. As for the third limit, thermal explosion has also been suggested to affect the overall explosion in an essential manner.[1,15,16] It is therefore clear that, in spite of the importance of the H_2-O_2 explosion phenomenon, there still exist aspects of it that require clarification and extension. Indeed, we shall show in due course that, through a systematic analysis, we are able to identify additional, rich insights into the characteristics and various system parameters affecting this supposedly well-studied phenomenon.

Before delving into the detailed exposition, it is instructive to first present a broad perspective of the explosion phenomena which we have acquired through the present study. Specifically, due to the competition between the strong low-pressure H-O_2 and the weak, high-pressure HO_2-H_2O_2 branched-chain mechanisms, the temperature-pressure plane is divided by the (extended) second limit into two domains, in which these two chain mechanisms, respectively, dominate, as shown in Fig. 1(a). Without any wall loss of the chain carriers, explosion occurs in both domains. When wall destruction is taken into consideration, each of them is further divided into an explosive subdomain and a non-explosive subdomain, as shown in Fig. 1(b). The three boundaries between the explosive and non-explosive domains are the three explosion limits. Consequently the efficiencies of the wall destruction of the five chain carriers, namely, H, O, OH, HO_2, and H_2O_2, relative

a)Author to whom correspondence should be addressed. Electronic mail: cklaw@princeton.edu

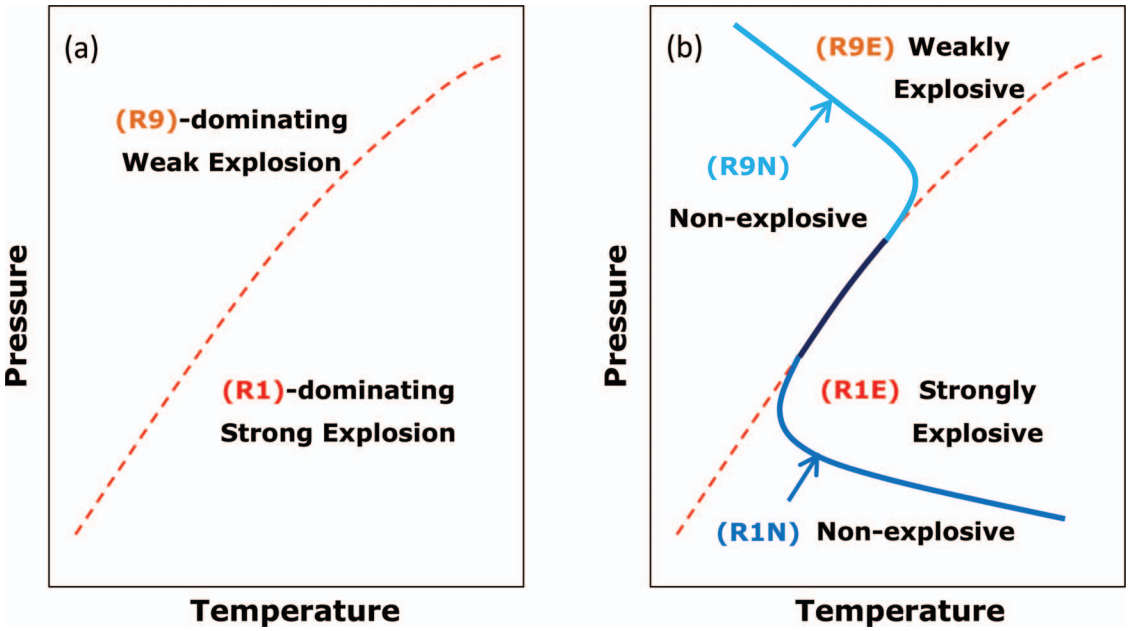

FIG. 1. The structure of the explosion limits according to the competing reaction mechanism analysis: (a) the backbone of the explosion limits, i.e., the extended second limit between (R1) and (R9) dominating domains without any wall destruction; (b) the first limit and the third limit, and the resulted second limit, due to wall destructions of the corresponding chain carriers.

to the gas-phase chain mechanisms as well as to each other, control the transitions in explosivity. Our study will therefore be concerned with the role of the relative efficiencies of the various reactions on the system response.

In Sec. II we shall first define the problem under study and assess the reactivity of the system by considering the competition between the different sub-mechanisms. In Sec. III the general explosion limits of the system are explored through an eigenvalue analysis, which is followed in Sec. IV by an examination of the relative importance of the wall destruction of the five chain carriers, identifying that the destructions of H and HO_2 are the key termination steps of the strong and weak branched-chain cycles. Based on this recognition and assuming gas-phase steadiness for O, OH, and H_2O_2, analytical results are obtained in Sec. V for the various explosion limits, including a cubic equation describing the complete Z-shaped response mentioned first by Semenov[17] and recently reported by Azatyan *et al.*[18] Using the analytical results of Sec. V, we perform in Sec. VI a general analysis of the loss of non-monotonicity in terms of the surface destruction efficiency and the hydrogen-oxygen molar fractions of the mixture. In the Appendix we present and analyze a model system of reactions mimicking the present one, leading to the derivation of a cubic equation describing the nonmonotonic phenomenon of triple explosion limits.

II. MODEL DEFINITION AND MECHANISM ANALYSIS

A. Assumptions and chemical mechanism

In order to identify the main features of the phenomenon of Z-shaped explosion limits, we base our study on the following two assumptions.

First, the process is treated as branched-chain explosion. According to the comprehensive kinetic models of the hydrogen-oxidation mechanism,[3,4] the system consists of eight species, namely, the reactants: H_2, O_2; the product: H_2O; and five chain-carrying intermediates (henceforth simply designated as carriers): H, O, OH, HO_2, and H_2O_2. At the very beginning stage of explosion, reactions between two carriers are infrequent and hence slow because of the low concentrations. Consequently only reactions between a carrier and a reactant are considered for the gas-phase reactions. Inclusion of reactions involving two carriers will render the system equations nonlinear and thereby immensely complicate the analysis. Furthermore, the concentrations of H_2 and O_2 as well as the temperature are assumed to be constant. By making the isothermal assumption, the role of reaction heat release and thereby the potential initiation of thermal runaway is not considered. Consequently, by subsequently showing that the Z-curve explosion limits can be adequately explained on the basis of carrier runaway, the reaction heat release is demonstrated to assume only a secondary role in the explosion limits.

Second, the kinetic approximation[1] is made in that diffusion of the carriers to the chamber wall is assumed to be much faster than wall absorption since only a small amount of the carriers that reach the wall are absorbed. Moreover, concentrations of the carriers at the wall are assumed to be the same as those in the gas phase. As such, the reactive system is treated to be spatially homogeneous.

The reaction mechanism consists of the chain initiation steps and six major chain reactions involving the carriers with H_2 or O_2, as shown in Table I. The kinetic parameters were taken from Ref. 19, recognizing nevertheless that, because of the general nature of the present study, the use of several alternate mechanisms recently published[20–22] is expected to yield similar results.

For simplicity, the rate constants for reactions (R9) and (R15) are computed, respectively, by $k_9 = [\mathrm{M}]^{-1}\{1/k_{9,\infty}$

TABLE I. The adopted H_2-O_2 chain reactions, with $k(T) = BT^{\alpha}e^{-E_a/(R^oT)}$.

No.	Reaction	B [cm,mol,s]	α	E_a (cal/mol)
(R1)	$H + O_2 \xrightarrow{k_1} O + OH$	1.04×10^{14}	0	15 286
(R2)	$O + H_2 \xrightarrow{k_2} H + OH$	3.82×10^{12}	0	7948
(R3)	$OH + H_2 \xrightarrow{k_3} H + H_2O$	2.17×10^{8}	1.52	3457
(R9)	$H + O_2 + M \xrightarrow{k_9} HO_2 + M$			
	$k_{9,\infty}$	5.59×10^{13}	0.2	0
	$k_{9,0}$	2.65×10^{19}	−1.3	0
(R17b)	$HO_2 + H_2 \xrightarrow{k_{17b}} H_2O_2 + H$	7.15×10^{4}	2.54	21 404
(R15)	$H_2O_2 + M \xrightarrow{k_{15}} 2OH + M$			
	$k_{15,\infty}$	8.59×10^{14}	0	48 560
	$k_{15,0}$	9.55×10^{15}	0	42 203

$+ 1/(k_{9,0}[M])\}^{-1}$ and $k_{15} = [M]^{-1}\{1/k_{15,\infty} + 1/(k_{15,0}[M])\}^{-1}$. Here, the fall-off parameters of all the third or second body species are assumed to be the same. Thus, for the stoichiometric H_2-O_2 mixture, we have $[M] = [H_2] + [O_2] = 3[O_2]$, i.e., $[O_2] = \xi_{O_2}[M]$ and $[H_2] = \xi_{H_2}[M]$ with $\xi_{H_2} = 2\xi_{O_2} = 2/3$. For the stoichiometric H_2-air mixture, O_2 has a molar fraction of 1/5 in the air and $\xi_{O_2} = 1/7$. Assuming ideal gas, the total gas concentration [M] is proportional to the total pressure, i.e., $[M] = p/(R^oT)$.

The carriers are destroyed at the wall according to the reactions,

$$H, O, OH, HO_2, H_2O_2 \xrightarrow{k_H, k_O, k_{OH}, k_{HO_2}, k_{H_2O_2}} \text{wall destruction},$$

with the equivalent reaction rate constants per unit volume k_H, k_O, k_{OH}, k_{HO_2}, and $k_{H_2O_2}$ given by[1]

$$k = \frac{1}{4}\varepsilon\bar{v}\frac{S}{V}. \quad (1)$$

Here, $\bar{v} = \sqrt{8k_BT/\pi m}$ is the average velocity of the thermal motion of the carriers at temperature T, m is the molar mass, and k_B is the Boltzmann constant. The sticking coefficient ε measures the destruction efficiency in the collision with the wall; usually $\varepsilon \approx 10^{-5}$ to 10^{-2} for glass and quartz.[1,2]

The main parameters that control whether the system explodes are the shape and size of the chamber, the wall sticking coefficients of the carriers, the temperature, total gas concentration, and molar fractions of hydrogen and oxygen. A spherical chamber is used, with diameter $2r = 0.074$ m and surface/volume ratio $S/V = 3/r$.

B. Explosion limits as the balance results of mechanism competitions

First, we investigate the structure of the Z-shaped explosion limits. Viewing it as the critical conditions of the branched-chain explosions, our interest is the chain character of the system.

There are two branched-chain mechanisms with the loop-starting reactions (R1) and (R9), respectively. The (R1)-starting chain includes the loops consisting of (R1)-(R2), (R1)-(R3), and (R1)-(R2)-(R3). The (R9)-starting branched-chain includes the loops consisting of (R9)-(R17b) and (R9)-(R17b)-(R15)-(R3). Consuming H atoms, the second-order reaction (R1) and the third-order reaction (R9) compete with each other. As a result, the two corresponding branched-chain mechanisms dominate at low and high pressures, respectively. They both produce chain carriers that may lead to explosion. On the other hand, the wall destruction of these chain carriers inhibits explosion.

The three explosion limits are, respectively, controlled by three corresponding groups of the competing reaction pairs, represented by the ratios of their reaction rate constants, namely, $\{k_1/k_9\}$ for the second limit, $\{k_H/k_1, k_O/k_2, k_{OH}/k_3\}$ for the first limit, and $\{k_{HO_2}/k_{17b}, k_{H_2O_2}/k_{15}, \sqrt{k_H/k_9}, k_{OH}/k_3\}$ for the third limit. Note that all the involved quantities have the dimension of concentration. For example, the backbone of the Z-shaped explosion limits, i.e., the asymptotic (extended) second explosion limit, is $[M] = 2k_1/k_9$.

The wall destruction of the five carriers plays different roles in controlling the explosion limits. The destruction of H and HO_2 are the key termination steps because they compete with (R1) and (R9)-(R17b), which are the primary sources for the two branched-chain cycles. As such, they must be included in a minimal reaction mechanism describing the Z-shaped explosion limits, and their respective roles are irreplaceable. For instance, without the wall destruction of HO_2, the destruction of H_2O_2 cannot balance the high-pressure chain cycle. Similarly, neither the wall destruction of O nor that of OH can individually balance the low-pressure chain cycle.

In addition to the qualitative differences for the wall destruction of the five carriers, the quantitative differences between them are also significant. For the first limit, it has been shown that it is possible to neglect the wall destruction of O and OH by comparing the ratios k_H/k_1 with k_O/k_2 and k_{OH}/k_3 due to the rates of the corresponding competing gas-phase reactions.[1] Similarly, owing to the very weak rate-limiting reactions (R17b) and (R15), the (R9) branched-chain explosion takes place only at high pressures in order to overcome the wall destruction of HO_2 and H_2O_2, while at those pressures the wall destructions of H and OH are negligible compared with their competing homogeneous reactions. This indicates that the wall destructions of HO_2 and H_2O_2 are the more efficient termination steps of the high-pressure chain cycle.

III. EIGENVALUE ANALYSIS

Based on the above considerations, the reaction rate equations for the carriers H, O, OH, HO_2, and H_2O_2 are given in matrix form by

$$\frac{d}{dt}\begin{bmatrix}[H]\\[O]\\[OH]\\[HO_2]\\[H_2O_2]\end{bmatrix} = A\begin{pmatrix}[H]\\[O]\\[OH]\\[HO_2]\\[H_2O_2]\end{pmatrix} + \begin{pmatrix}I\\0\\0\\I\\0\end{pmatrix}, \quad (2)$$

where $I = k_I[O_2][H_2]$ is the rate of the chain initiation reaction $H_2 + O_2 \rightarrow HO_2 + H$, and

$$\mathrm{A} = \begin{bmatrix} -k_1[\mathrm{O_2}] - k_9[\mathrm{O_2}][\mathrm{M}] - k_\mathrm{H} & k_2[\mathrm{H_2}] & k_3[\mathrm{H_2}] & k_{17b}[\mathrm{H_2}] & 0 \\ k_1[\mathrm{O_2}] & -k_2[\mathrm{H_2}] - k_\mathrm{O} & 0 & 0 & 0 \\ k_1[\mathrm{O_2}] & k_2[\mathrm{H_2}] & -k_3[\mathrm{H_2}] - k_\mathrm{OH} & 0 & 2k_{15}[\mathrm{M}] \\ k_9[\mathrm{O_2}][\mathrm{M}] & 0 & 0 & -k_{17b}[\mathrm{H_2}] - k_{\mathrm{HO_2}} & 0 \\ 0 & 0 & 0 & k_{17b}[\mathrm{H_2}] & -k_{15}[\mathrm{M}] - k_{\mathrm{H_2O_2}} \end{bmatrix}. \quad (3)$$

For such a linear system, whether explosion takes place depends on the real part of the eigenvalues of the coefficient matrix A. If any of the eigenvalues has a positive real part, the intermediate concentrations will increase exponentially with time, leading to branched-chain explosion. Otherwise, there is no explosion. Therefore, the explosion limits, defined as the boundaries between the explosive and the non-explosive domains in the temperature-concentration (or temperature-pressure) diagram, are given by the neutral condition $\zeta(T, [\mathrm{M}]) = 0$, or equivalently $\zeta(T, p/(R^oT)) = 0$, where ζ denotes the largest real part of the eigenvalues.

A. Role of hydrogen vs. oxygen concentrations

We first study effects of the relative concentrations of hydrogen and oxygen on the explosion limits. For mixtures without any inert, Fig. 2(a) shows that, with a smaller molar fraction of hydrogen, which correspondingly implies a larger molar fraction of oxygen, the system is more explosive near the first limit and less explosive near the third limit. The reason is that oxygen is involved in the rate-limiting step of the low-pressure branched-chain, namely, reaction (R1), while hydrogen is involved in reaction (R17b) of the high-pressure branched-chain. As a result, it is more effective to render a mixture more explosive by adding oxygen at low pressures and by adding hydrogen at high pressures. The converse holds from explosion safety considerations.

For hydrogen-oxygen mixtures diluted with an inert gas, the total molar concentration is $[\mathrm{M}] = [\mathrm{H_2}] + [\mathrm{O_2}] + [\mathrm{Inert}]$. Figure 2(b) shows that the explosion limits of stoichiometric hydrogen-oxygen-inert gas mixtures, in which the corresponding molar ratios $[\mathrm{H_2}]$: $[\mathrm{O_2}]$: [Inert] are marked. For instance, for a stoichiometric hydrogen-air mixture, it is about 2:1:4. It is then seen that with a larger inert addition, the mixture is less explosive because of the reduced effective concentrations.

B. Structure: The low-pressure explosion peninsula (R1E) and the high-pressure no-explosion peninsula (R9N)

At low pressures sufficiently remote from the third limit, the wall destruction of $\mathrm{HO_2}$ and $\mathrm{H_2O_2}$ predominate over their gas-phase reactions (R17b) and (R15), respectively. In this case, $k_{17b}[\mathrm{H_2}] \ll k_{\mathrm{HO_2}}$, $k_{15}[\mathrm{M}] \ll k_{\mathrm{H_2O_2}}$. Therefore, in the low-pressure limit with these terms ignored in the characteristic equation, matrix (3) has the same eigenvalues as

$$\mathrm{A_{LP}} = \begin{bmatrix} -k_1[\mathrm{O_2}] - k_9[\mathrm{O_2}][\mathrm{M}] - k_\mathrm{H} & k_2[\mathrm{H_2}] & k_3[\mathrm{H_2}] & 0 & 0 \\ k_1[\mathrm{O_2}] & -k_2[\mathrm{H_2}] - k_\mathrm{O} & 0 & 0 & 0 \\ k_1[\mathrm{O_2}] & k_2[\mathrm{H_2}] & -k_3[\mathrm{H_2}] - k_\mathrm{OH} & 0 & 0 \\ k_9[\mathrm{O_2}][\mathrm{M}] & 0 & 0 & -k_{\mathrm{HO_2}} & 0 \\ 0 & 0 & 0 & 0 & -k_{\mathrm{H_2O_2}} \end{bmatrix}. \quad (4)$$

It is easy to find that the five eigenvalues of matrix (4) are $-k_{\mathrm{HO_2}}$, $-k_{\mathrm{H_2O_2}}$ and three additional ones corresponding to the eigenvalues of the following degenerate system:

$$\mathrm{A_{LP}}' = \begin{bmatrix} -k_1[\mathrm{O_2}] - k_9[\mathrm{O_2}][\mathrm{M}] - k_\mathrm{H} & k_2[\mathrm{H_2}] & k_3[\mathrm{H_2}] \\ k_1[\mathrm{O_2}] & -k_2[\mathrm{H_2}] - k_\mathrm{O} & 0 \\ k_1[\mathrm{O_2}] & k_2[\mathrm{H_2}] & -k_3[\mathrm{H_2}] - k_\mathrm{OH} \end{bmatrix}. \quad (5)$$

In this case, the three-body reaction (R9) acts as the gas-phase termination of the (R1) branched-chain, and $\zeta_{\mathrm{LP}}(T, p/(R^oT)) = 0$ yields the boundary of the low-pressure explosion peninsula (R1E).

At high pressures sufficiently remote from the first limit, the wall destruction of H, O, and OH are negligible compared with their competing reactions. Therefore, the boundary of the high-pressure no-explosion peninsula (R9N) is determined by

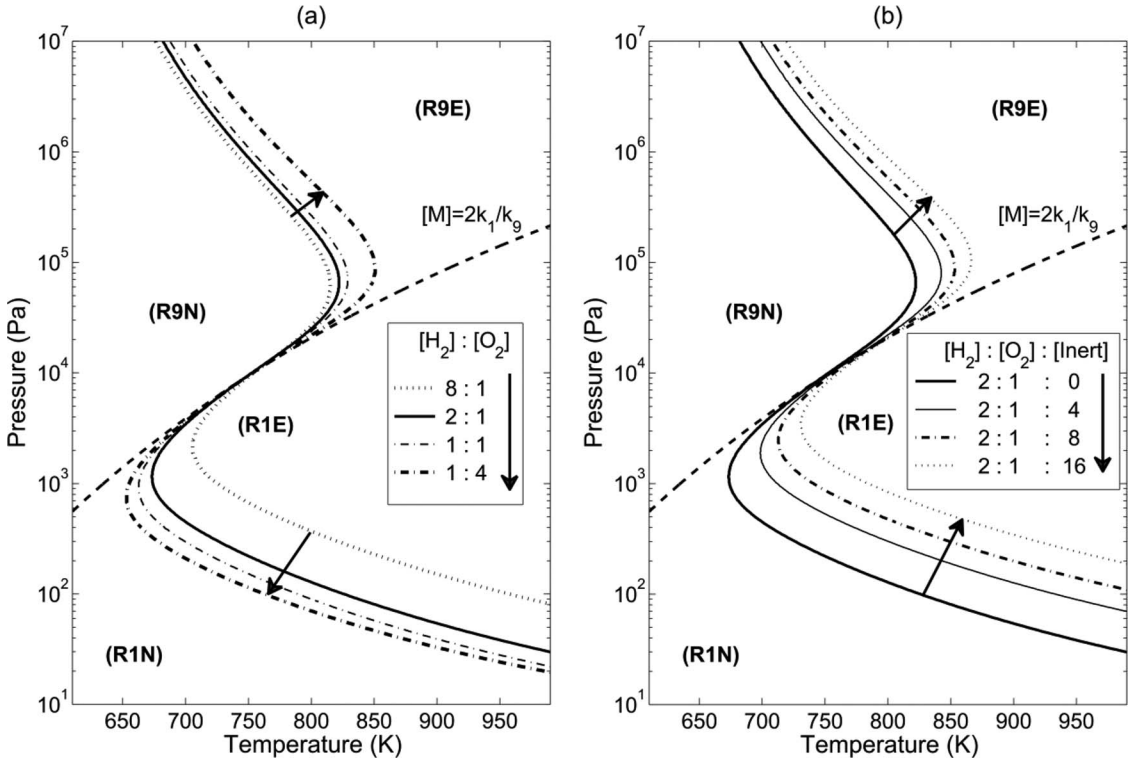

FIG. 2. Explosion limits of: (a) non-stoichiometric pure hydrogen-oxygen mixtures and (b) stoichiometric hydrogen-oxygen mixtures with inert gas. The corresponding molar ratios are marked. The sticking coefficients are: $\varepsilon_{\mathrm{H}} = \varepsilon_{\mathrm{O}} = \varepsilon_{\mathrm{OH}} = 10^{-3}$, $\varepsilon_{\mathrm{HO_2}} = 3 \times 10^{-3}$, and $\varepsilon_{\mathrm{H_2O_2}} = 3 \times 10^{-4}$.

the neutral condition $\zeta_{\mathrm{HP}}(T, p/(R^o T)) = 0$ with $k_{\mathrm{H}} = 0$, $k_{\mathrm{O}} = 0$, and $k_{\mathrm{OH}} = 0$, i.e., for

$$\mathrm{A_{HP}} = \begin{bmatrix} -k_1[\mathrm{O_2}] - k_9[\mathrm{O_2}][\mathrm{M}] & k_2[\mathrm{H_2}] & k_3[\mathrm{H_2}] & k_{17b}[\mathrm{H_2}] & 0 \\ k_1[\mathrm{O_2}] & -k_2[\mathrm{H_2}] & 0 & 0 & 0 \\ k_1[\mathrm{O_2}] & k_2[\mathrm{H_2}] & -k_3[\mathrm{H_2}] & 0 & 2k_{15}[\mathrm{M}] \\ k_9[\mathrm{O_2}][\mathrm{M}] & 0 & 0 & -k_{17b}[\mathrm{H_2}] - k_{\mathrm{HO_2}} & 0 \\ 0 & 0 & 0 & k_{17b}[\mathrm{H_2}] & -k_{15}[\mathrm{M}] - k_{\mathrm{H_2O_2}} \end{bmatrix}. \quad (6)$$

The above two limits, respectively, constitute a low-pressure explosion-limit peninsula and a high-pressure explosion-limit peninsula, as shown in Fig. 3. The asymptotic second limit $[\mathrm{M}] = 2k_1/k_9$, i.e., the backbone, divides the temperature-pressure plane into the (R1) and (R9) branched-chain dominating domains, which are in turn divided into explosion and no-explosion subdomains by the first and third limits, as anticipated in Fig. 1. These constitute the structure analysis.

IV. ROLE OF THE WALL DESTRUCTION OF THE CHAIN CARRIERS

A. Key roles of the destruction of H and HO_2

We first investigate the roles of the wall destruction of H, O, and OH in controlling the low-pressure, first limit. In Fig. 4, we plot the explosion limits with the wall destruction of only one of them, while allowing for the destruction of HO_2 and H_2O_2. It is seen that in the case involving only the wall destruction of H, we obtain the first limit and thus the Z-shaped explosion limits. On the contrary, there is no first limit in cases involving the destruction of O or OH individually, even with a sticking coefficient of 1, as shown in the subplots (b) and (c). However, destruction of both of them together can balance the low-pressure branched-chain, although at a much lower efficiency as compared to that of H.

Similarly, only the wall destruction of H_2O_2 individually cannot terminate the high-pressure branched-chain, while that of HO_2 satisfactorily exhibits the second and the third explosion limits, as shown in Fig. 5.

Consequently, the wall destructions of H and HO_2 are the key termination steps of the low-pressure and high-pressure branched-chains, respectively, such that a minimal

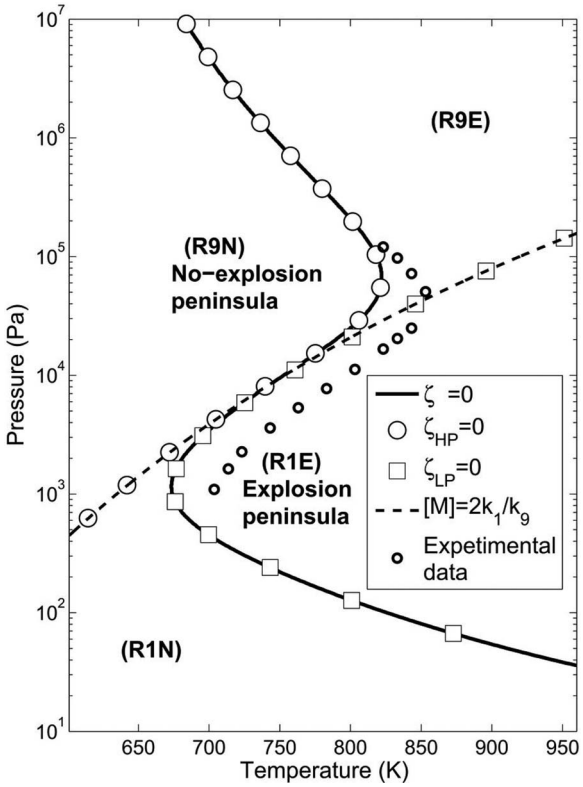

FIG. 3. Explosion limits of a stoichiometric hydrogen-oxygen mixture in a spherical KCl-coated vessel of 7.4 cm diameter. The open cycles are the experimental data abstracted from Ref. 2. The solid Z-shaped curve is obtained by the eigenvalue analysis with the sticking coefficients: $\varepsilon_H = \varepsilon_O = \varepsilon_{OH} = 10^{-3}$, $\varepsilon_{HO_2} = 3 \times 10^{-3}$, and $\varepsilon_{H_2O_2} = 3 \times 10^{-4}$.

mechanism incorporating them will exhibit the Z-shaped explosion limits. As shown in Fig. 6, $\zeta_{H,HO_2}(T, [M]) = 0$ is Z-shaped, although it is slightly more explosive than the comprehensive one with the destruction of all the five carriers, especially for the third limit.

The key roles of the wall destruction of H and HO_2 are also implied by the approximate analytical explosion limits. For instance, in the low-pressure limit, by ignoring the three-body reaction term in matrix (5) and assuming quasi-steadiness for O and OH, one can obtain the asymptotic first limit determined by[1] $-k_H + k_1[O_2]\{-1 + \frac{k_3[H_2]}{k_{OH}+k_3[H_2]} + \frac{k_2[H_2]}{k_O+k_2[H_2]}(1 + \frac{k_3[H_2]}{k_{OH}+k_3[H_2]})\} = 0$. In the case involving only the wall destruction of H, $-k_H + 2k_1[O_2] = 0$ determines $[O_2] = k_H/2k_1$. However, involving only the wall destruction of OH instead, the resulting neutral equation $k_1[O_2]\frac{2k_3[H_2]}{k_{OH}+k_3[H_2]} = 0$ has no positive concentration root to yield the first limit, in contrast to the statement in Ref. 3. Similarly, the wall destruction of O alone cannot balance the (R1) branched-chain, and that of H_2O_2 alone cannot explain the third limit. Therefore, the wall destructions of them are only supplementary to those of H and HO_2, which are the essential ones determining the Z-shaped response.

B. Qualitative effects of the wall destruction of the chain carriers

With larger wall sticking coefficients of the H radical, the first limit moves to higher pressure and higher temperature regimes along the backbone second limit, as shown in Fig. 7(a). Similarly, with larger sticking coefficients of HO_2, the third limit moves to higher *T-p* regime along the backbone. Furthermore, in cases with very large ε_H or very small ε_{HO_2}, the explosion boundary is not Z-shaped any more. We shall return to this issue in Sec. VI.

To investigate the quantitative effects of the wall destruction of OH, O, and H_2O_2, we have plotted the explosion limits with them in addition to those of H and HO_2 as dashed lines in Fig. 7. It is seen that with the same sticking coefficient as H, the additional wall destructions of OH and O affect the first limit slightly in Fig. 7(a), whereas that of H_2O_2 pushes the third limit higher significantly with it having the same sticking coefficient as that of HO_2, in Fig. 7(b). The large differences in the termination efficiency among these wall destructions are due to the different rates of the competing homogeneous reactions.

In summary, the explosion limits are sensitively controlled by the wall destruction, especially those of H and HO_2. Either wall destructions of the more reactive kinds or with higher destruction efficiencies render the system less explosive, which is reasonable. More specifically, the first limit and the lower turning point are controlled mainly by the destruction efficiency of H. The third limit and the upper turning point are controlled mainly by those of HO_2 and H_2O_2. It is also noted that under certain experimental conditions, the vessel wall is far less destructive for H_2O_2 than it is for HO_2, i.e., $k_{H_2O_2} \ll k_{HO_2}$.[2] In these cases, the explosion limits are controlled by the wall destruction efficiencies of H and HO_2.

V. A CUBIC EQUATION FOR THE EXPLOSION LIMITS

Utilizing the above insights that the wall destructions of the carriers are dominated by those of H and HO_2, we identify a system that is both realistic and also amenable to analyticity.

A. The general cubic equation for the three limits

With H and HO_2 being the only carriers destroyed at the wall, and further assuming quasi-steadiness for O, OH, and H_2O_2, the evolution of H and HO_2 is governed by

$$\frac{d}{dt}\begin{pmatrix}[H]\\[HO_2]\end{pmatrix} = A_{H,HO_2}\begin{pmatrix}[H]\\[HO_2]\end{pmatrix} + \begin{pmatrix}I\\I\end{pmatrix}, \tag{7}$$

with the coefficient matrix given by

$$A_{H,HO_2} = \begin{bmatrix} 2k_1[O_2] - k_9[O_2][M] - k_H & 3k_{17b}[H_2] \\ k_9[O_2][M] & -k_{17b}[H_2] - k_{HO_2} \end{bmatrix}. \tag{8}$$

The neutral condition is then determined through

$$(2k_1[O_2] - k_9[O_2][M] - k_H)(-k_{17b}[H_2] - k_{HO_2}) - (3k_{17b}[H_2])(k_9[O_2][M]) = 0, \tag{9}$$

with $k_9 = [M]^{-1}\{1/k_{9,\infty} + 1/(k_{9,0}[M])\}^{-1}$.

After some manipulation, Eq. (9) can be expressed as a cubic equation for the critical concentration (pressure),

$$f_{H,HO_2}(T, [M]) = a(T)[M]^3 + b(T)[M]^2 + c(T)[M] + d(T) = 0, \tag{10}$$

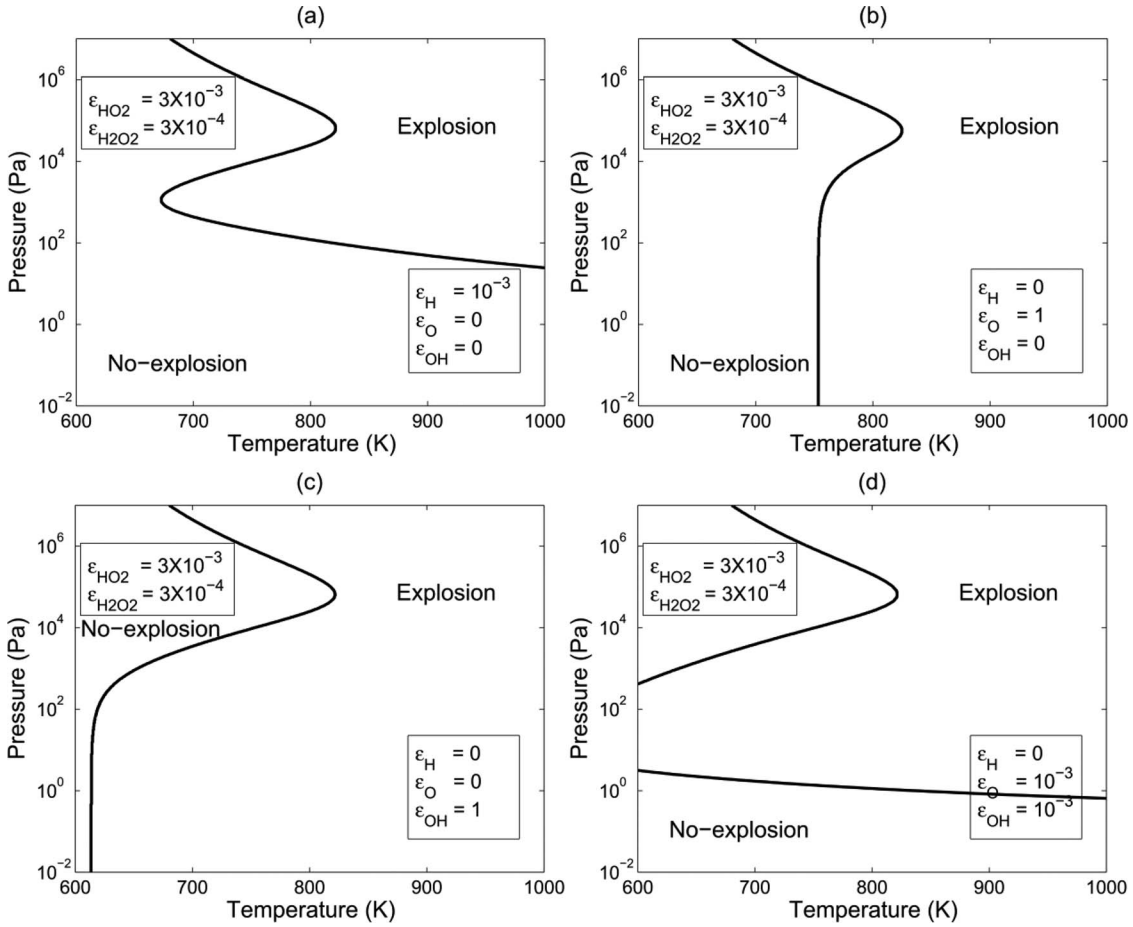

FIG. 4. Explosion limits with wall destruction of: (a) H with $\varepsilon_H = 10^{-3}$; (b) O with $\varepsilon_O = 1$; (c) OH with $\varepsilon_{OH} = 1$; and (d) both O and OH with $\varepsilon_O = \varepsilon_{OH} = 10^{-3}$ for the low-pressure branched-chain. For the termination steps of the high-pressure branched-chain, the additional sticking coefficients are $\varepsilon_{HO_2} = 3 \times 10^{-3}$ and $\varepsilon_{H_2O_2} = 3 \times 10^{-4}$.

whose coefficients depend on the temperature, with the molar fractions and the sticking coefficients being the system parameters,

$$a(T) = 2\xi_{H_2}\xi_{O_2}\left(1 + \frac{k_1}{k_{9,\infty}}\right),$$

$$b(T) = \xi_{O_2}\frac{k_{HO_2}}{k_{17b}}\left(2\frac{k_1}{k_{9,\infty}} - 1\right) - \xi_{H_2}\frac{k_H}{k_{9,\infty}} + 2\xi_{H_2}\xi_{O_2}\frac{k_1}{k_{9,0}},$$

$$c(T) = 2\xi_{O_2}\frac{k_1}{k_{9,0}}\frac{k_{HO_2}}{k_{17b}} - \xi_{H_2}\frac{k_H}{k_{9,0}} - \frac{k_H}{k_{9,\infty}}\frac{k_{HO_2}}{k_{17b}}, \quad \text{and}$$

$$d(T) = -\frac{k_H}{k_{9,0}}\frac{k_{HO_2}}{k_{17b}}.$$

With typical values of the molar fractions and sticking coefficients, the positive real roots of the cubic equation (10)

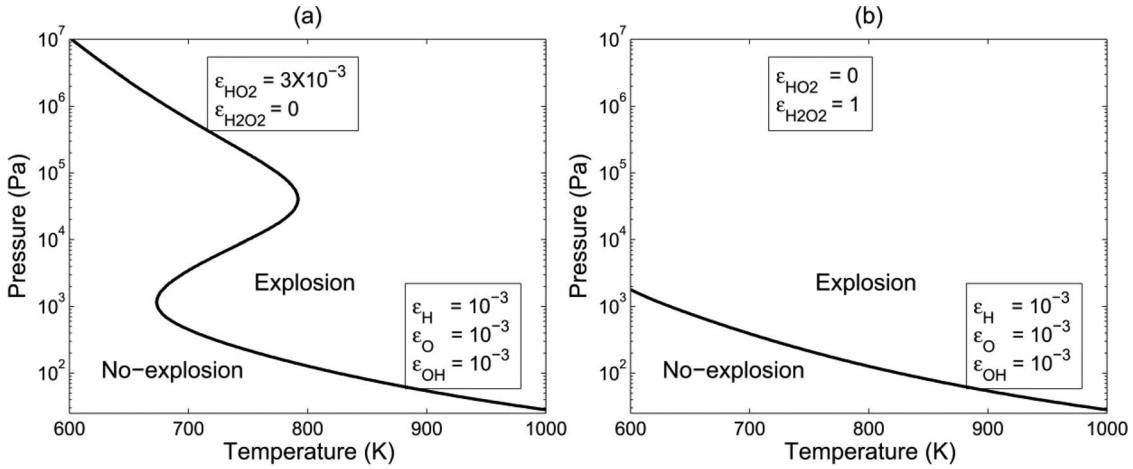

FIG. 5. Explosion limits with wall destruction of: (a) $\varepsilon_{HO_2} = 3 \times 10^{-3}$ and (b) $\varepsilon_{H_2O_2} = 1$ for the high-pressure branched-chain. For the termination steps of the low-pressure branched-chain, the additional sticking coefficients are $\varepsilon_H = \varepsilon_O = \varepsilon_{OH} = 10^{-3}$.

yield the Z-shaped explosion limits. At very low or very high temperatures, the cubic equation has only one positive real root. At intermediate temperatures, it has three distinct positive real roots. Furthermore, at each of two critical temperatures, it has one simple real root and one double real root, indicating the state of the turning point. The nature of the roots can be determined by computing the discriminant of the cubic equation (10), namely, $\Delta = abcd - 4b^3d + b^2c^2 - 4ac^3 - 27a^2d^2$ (Ref. 23).

We note in passing that while Eq. (10) was derived independently herein, the same result was reported earlier, in Ref. 18.

B. The degenerate (two-limit) quadratic and (single-limit) linear equations

From the above results, the low-pressure explosion peninsula is determined by $2k_1[O_2] - k_9[O_2][M] - k_H = 0$ from Eq. (9) for $k_{17b}[H_2] \ll k_{HO_2}$, with the three terms, respectively, representing branching, gas-phase termination through (R9), and wall termination of H. This yields an explicit quadratic expression given by

$$\left(1 - \frac{2k_1}{k_{9,\infty}}\right)[M]^2 - \left(\frac{2k_1}{k_{9,0}} - \frac{k_H}{\xi_{O_2}k_{9,\infty}}\right)[M] + \frac{k_H}{\xi_{O_2}k_{9,0}} = 0.$$

The above result can be further simplified by using the (realistic) relations $\frac{k_1}{k_{9,\infty}} \ll 1$ and $\frac{k_H}{k_1}\frac{k_{9,0}}{k_{9,\infty}} \ll 1$, yielding

$$[M]^2 - \frac{2k_1}{k_{9,0}}[M] + \frac{k_H}{\xi_{O_2}k_{9,0}} = 0. \quad (11)$$

This is the same expression as that of Ref. 1 for $k_9 = k_{9,0}$.

It is of interest to note that the above expression (11) can also be obtained by invoking an alternate set of assumptions. That is, using the cubic equation (10) and the (realistic) relations $\frac{k_1}{k_{9,\infty}} \ll 1$, $\frac{k_H}{k_1}\frac{k_{9,0}}{k_{9,\infty}} \ll 1$, $\frac{k_H}{k_{9,\infty}} \ll \frac{k_{HO_2}}{k_{17b}}$, and $\frac{k_H}{k_1} \ll \frac{k_{HO_2}}{k_{17b}}$, we obtain

$$a(T) \approx 2\xi_{H_2}\xi_{O_2}, \quad b(T) \approx -\xi_{O_2}\frac{k_{HO_2}}{k_{17b}}, \quad \text{and}$$

$$c(T) \approx 2\xi_{O_2}\frac{k_1}{k_{9,0}}\frac{k_{HO_2}}{k_{17b}},$$

which reduce Eq. (10) to $2\xi_{H_2}\xi_{O_2}[M]^3 - \xi_{O_2}\frac{k_{HO_2}}{k_{17b}}([M]^2 - \frac{2k_1}{k_{9,0}}[M] + \frac{k_H}{\xi_{O_2}k_{9,0}}) = 0$, which in turn is further simplified to Eq. (11) for $[M] \ll \frac{k_{HO_2}}{k_{17b}}$.

Similarly, the high-pressure no-explosion peninsula is determined by

$$2k_1[O_2] + \left(\frac{3k_{17b}[H_2]}{k_{HO_2} + k_{17b}[H_2]} - 1\right)k_9[O_2][M] = 0,$$

from Eq. (9) by ignoring the destruction of H, with the three terms, respectively, representing the effects of low-pressure branching, high-pressure branching, and wall termination of HO_2. This expression can be rearranged to

$$2k_1 = \frac{-k_{HO_2} + 2k_{17b}[H_2]}{k_{HO_2} + k_{17b}[H_2]}k_9[M]. \quad (12)$$

Equation (12) is different from the result: $2k_1 = \frac{k_{HO_2}}{k_{HO_2}+k_{17b}[H_2]}k_9[M]$, given by Ref. 2, which does not account for the competition between the high-pressure branched-chain and the wall destruction of HO_2.

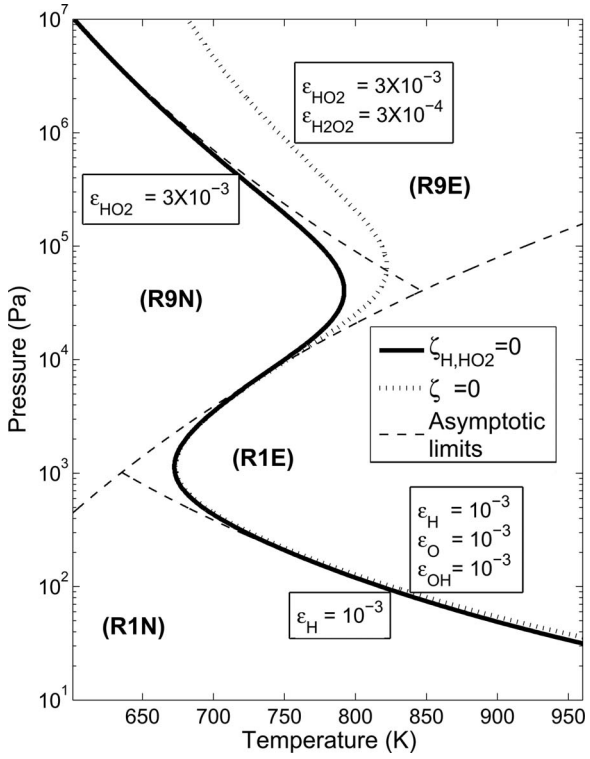

FIG. 6. The Z-shaped explosion limits involving only the wall destruction of H and HO_2, as the solid curve. The sticking coefficients are $\varepsilon_H = 10^{-3}$ and $\varepsilon_{HO_2} = 3 \times 10^{-3}$. The dotted line involves the destruction of all chain carriers with the additional sticking coefficients $\varepsilon_O = \varepsilon_{OH} = 10^{-3}$ and $\varepsilon_{H_2O_2} = 3 \times 10^{-4}$. The three dashed lines are the asymptotic limits obtained by approximate quasi-steady-state analysis.

Furthermore, from the (two-limit) quadratic equations (11) and (12), the three asymptotic explosion limits can be determined. Specifically, at the high temperature range where $\frac{k_H}{\xi_{O_2}k_1} / \frac{k_1}{k_{9,0}} \le 1$, Eq. (11) has two roots, representing the two asymptotic explosion limits $[M]_{1st} \approx \frac{k_H}{2\xi_{O_2}k_1}$ and $[M]_{2nd} \approx \frac{2k_1}{k_{9,0}}$, which were first obtained by Semenov.[1] Similarly, $[M]_{3rd} \approx \frac{k_{HO_2}}{2\xi_{H_2}k_{17b}}$ and $[M]_{2nd} \approx \frac{2k_1}{k_{9,0}}$ can be obtained from Eq. (12).

Alternatively, the three asymptotic explosion limits can also be determined directly from the cubic equation (10). For instance, in the low-pressure limit, balance between the two dominant terms, i.e., $c(T)[M] + d(T) = 0$ determines the asymptotic first limit, $[M]_{1st} = -\frac{d(T)}{c(T)} \approx \frac{k_H}{2\xi_{O_2}k_1}$. These three asymptotic limits are in good agreement with the full eigenvalue analysis result, as shown in Fig. 6.

We close this section by noting that, strictly speaking, H_2O_2 is not a quasi-steady-state species according to the rates of corresponding production and consumption reactions. Nevertheless, this assumption facilitates understanding of the qualitatively different roles of the wall destruction of the five carriers in controlling the explosion limits.

VI. LOSS OF NON-MONOTONICITY

A. Transition criterion

Figure 7 shows that the explosion limits fail to exhibit non-monotonicity, namely, the Z-shaped response, for

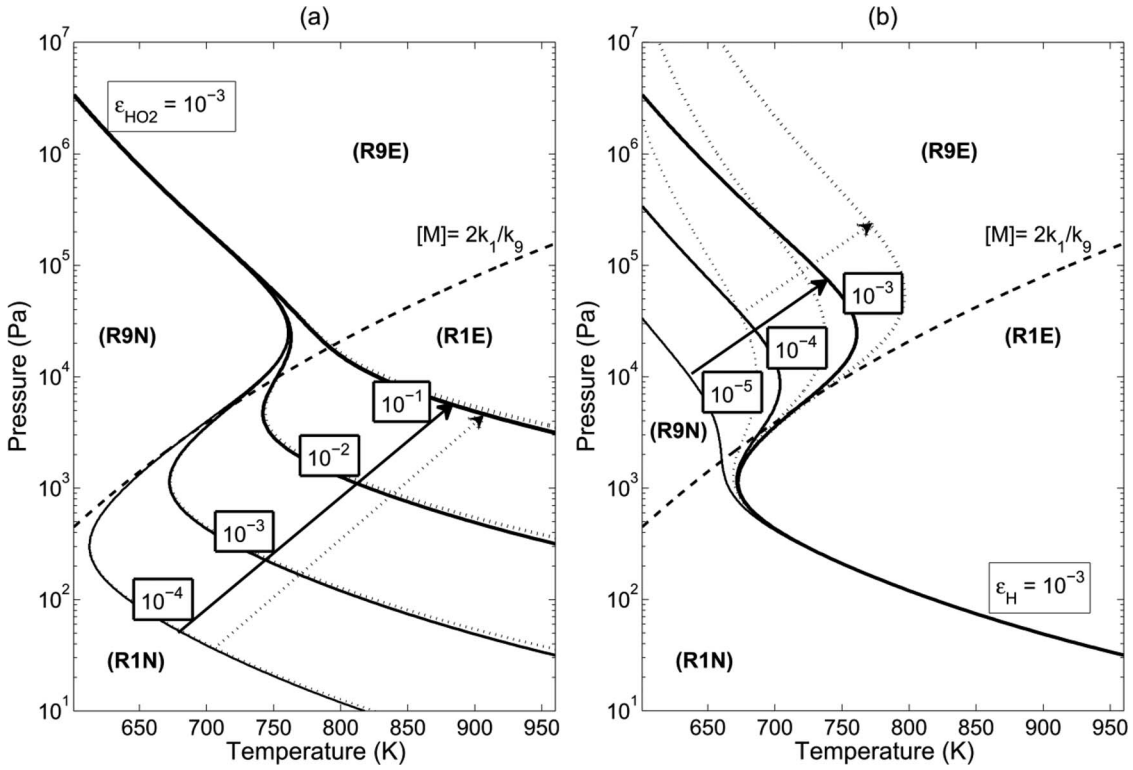

FIG. 7. Explosion limits involving the wall destruction of various chain carriers with different absorption efficiencies. The solid lines represent destruction of H and HO_2 only. The dotted lines represent additional destruction of: (a) OH and O with the same sticking coefficients as that of H and (b) H_2O_2 with the same sticking coefficients as that of HO_2. The corresponding sticking coefficients are marked.

some of the pure stoichiometric hydrogen-oxygen mixtures. We now consider the general criterion on the loss of non-monotonicity, using the mechanism represented by Eq. (10).

For the Z-shaped explosion limits with typical values of the parameters used above, over a narrow range of intermediate temperatures, there are three distinct positive [M] roots, which requires $\Delta > 0$ for three distinct real roots. Furthermore, $b < 0$, $c > 0$, and $d < 0$ are required so that all the three roots are positive. The two turning points correspond to the two positive double real roots of the cubic equation, namely, $\Delta = 0$ is satisfied at the two "turning temperatures," T_ℓ and T_h. In general, these two turning temperatures, with their corresponding turning pressures, depend only on the system parameters, namely, the molar fractions and the sticking coefficients.

For the pure hydrogen-oxygen system ($\xi_{H_2} + \xi_{O_2} = 1$) with the given sticking coefficients $\varepsilon_H = 10^{-3}$ and $\varepsilon_{HO_2} = 10^{-4}$, we plot in Fig. 8 the two turning temperatures for different values of the hydrogen molar fraction ξ_{H_2}. It is seen that, for the stoichiometric case, $\xi_{H_2} = 2/3$, the lower and the upper turning temperatures are about 670 K and 710 K, respectively. With higher molar fractions of hydrogen, corresponding to lower oxygen molar fractions, the lower turning temperature is higher, while the higher turning temperature is lower. Hence, the range of the second limit is reduced. As the molar fraction of hydrogen reaches a critical value, designated by the subscript "C," such that $T_\ell = T_h = T_C$, the second limit degenerates to a single point in the T-p plane. With further increase of the hydrogen molar fraction, the explosion limits lose the second limit and hence the Z-shape. The value of the corresponding critical molar fraction of hydrogen, $\xi_{H_2,C}$, depends only on the two sticking coefficients and hence is a fundamental parameter of the pure hydrogen-oxygen system. $\xi_{H_2,C}$ is about 0.91 for $\varepsilon_H = 10^{-3}$ and $\varepsilon_{HO_2} = 10^{-4}$, and is about 0.6 for $\varepsilon_H = 10^{-3}$ and $\varepsilon_{HO_2} = 10^{-5}$, as shown in Figs. 8 and 9.

It is important to recognize that, since the backbone second limit anchors the low- and high-pressure peninsulas, the loss of non-monotonicity for the two turning points occurs simultaneously.

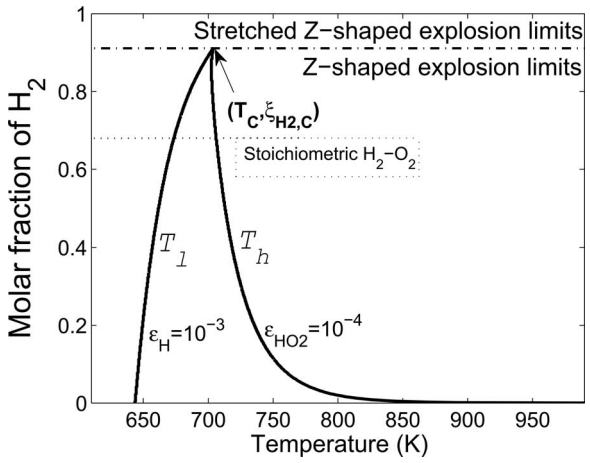

FIG. 8. The temperatures T_ℓ and T_h at the two turning points of the Z-shaped explosion limits dependent as functions of the molar fraction of hydrogen in pure hydrogen-oxygen mixtures, with the sticking coefficients $\varepsilon_H = 10^{-3}$ and $\varepsilon_{HO_2} = 10^{-4}$.

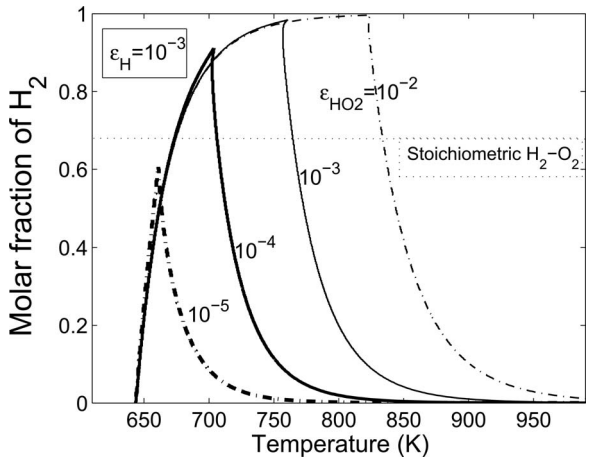

FIG. 9. The two turning-point temperatures as functions of the molar fraction of hydrogen in pure hydrogen-oxygen mixtures. The two sticking coefficients are: $\varepsilon_{\mathrm{H}} = 10^{-3}$, and $\varepsilon_{\mathrm{HO_2}} = 10^{-5}$, 10^{-4}, 10^{-3}, and 10^{-2}.

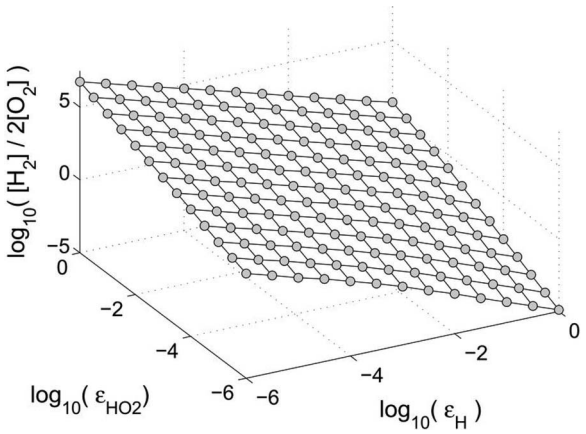

FIG. 11. Critical surface in the parameter space for the Z-shaped explosion limits for pure hydrogen-oxygen mixtures. The explosion limits are Z-shaped below the critical hydrogen-oxygen concentration ratio. Otherwise, the explosion limits are stretched.

B. Determination of the critical molar fraction with given sticking coefficients

Given the sticking coefficients, the critical state $(T_{\mathrm{C}}, \xi_{\mathrm{H_2,C}})$ can be determined by the intersection of the two lines, respectively, described by $b^2 - 3ac = 0$ and $c^2 - 3bd = 0$ in the temperature-molar fraction diagram, again together with $c > 0$, $b < 0$, and $d < 0$. In fact, the critical condition corresponds to the case when the cubic equation has a triple solution $[\mathrm{M}]_{\mathrm{triple}} = -b/3a = -c/b = -3d/c$. Therefore, the coefficients satisfy $b^2 - 3ac = 0$ and $c^2 - 3bd = 0$. In the temperature-pressure (concentration) diagram, the critical triple root is always located on the asymptotic second limit, and moves along it when the system parameters change.

C. Critical surface in the parameter space

For pure hydrogen-oxygen mixtures, the critical molar fraction and the critical temperature are shown in Fig. 10 as functions of the sticking coefficients. It is observed that the critical molar fraction of hydrogen decreases with increasing ε_{H} and increases with increasing $\varepsilon_{\mathrm{HO_2}}$. The corresponding critical temperature increases with both ε_{H} and $\varepsilon_{\mathrm{HO_2}}$. Below the critical molar fraction of hydrogen, the explosion limits are Z-shaped. Above the critical molar fraction, the explosion limits lose non-monotonicity. Therefore, increasing the sticking coefficient $\varepsilon_{\mathrm{HO_2}}$ and decreasing the sticking coefficient ε_{H} widen the range of the molar fraction of hydrogen for the Z-shaped explosion limits. In the log-log-log plot (Fig. 11), where the hydrogen/oxygen concentration ratio is used instead of the molar fraction of hydrogen, the critical parameter surface is almost a plane.

More generally, for any hydrogen-oxygen mixtures consisting of an inert, we have an additional independent controlling parameter, that is, the molar fraction of the inert. Take as an example the hydrogen-air mixture, with $[\mathrm{O_2}]$: [Inert] = 1: 4, shown in Fig. 12(b). Given the molar fraction and the sticking coefficient ε_{H}, one can obtain the critical value of $\varepsilon_{\mathrm{HO_2}}$, which increases with both $\xi_{\mathrm{H_2}}$ and ε_{H}. In the log-log plot, the dependences are almost linear.

In summary, the parameter space of the molar fractions and the sticking coefficients are partitioned by a critical surface into two domains, in which the explosion limits are, respectively, multiple valued in the form of a Z shape, and

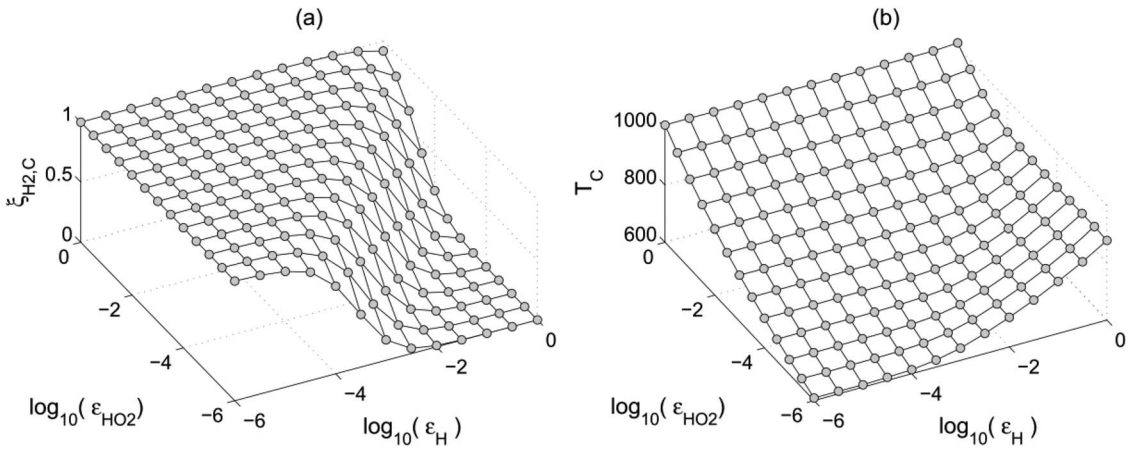

FIG. 10. Critical values for the Z-shaped explosion limits for pure hydrogen-oxygen mixtures: (a) critical molar fraction of hydrogen and (b) the corresponding critical temperature. The explosion limits are Z-shaped below the critical molar fraction of hydrogen. Otherwise, the explosion limits are stretched.

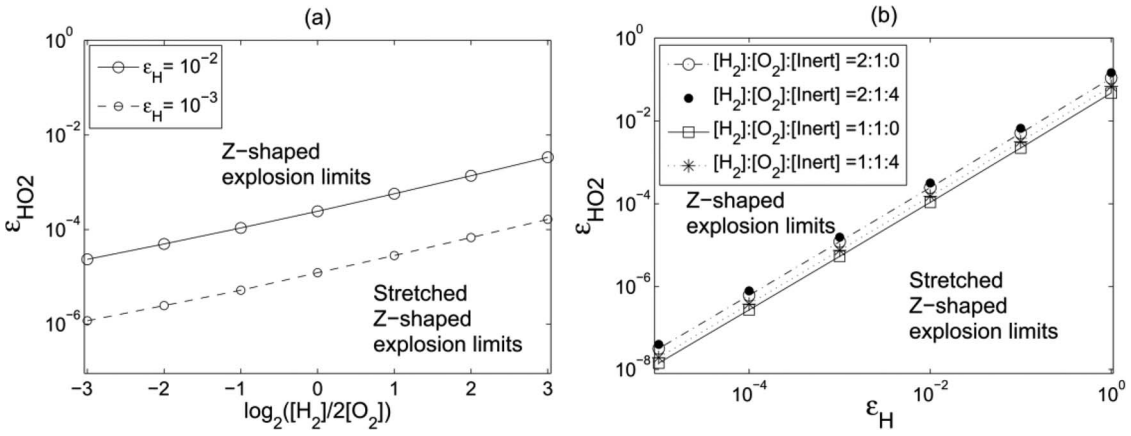

FIG. 12. Dependence of the critical ε_{HO_2} on: (a) the hydrogen-oxygen concentration ratio and (b) ε_H.

single valued, respectively. These are the results of the relative strengths of the competition between the two branched-chains and their respective terminations.

VII. CONCLUDING REMARKS

In this study, we have analyzed the explosion limits of hydrogen-oxygen mixtures.

The structure of the explosion limits of hydrogen-oxygen mixtures is explored through a rational analysis, which allows further insightful interpretation, as follows. As results of the three reaction mechanism competitions, namely, the competition between the low- and high-pressure branched-chains and those between them and the respective wall terminations, the temperature-pressure plane is first divided into the (R1)- and the (R9)-dominating domains, which are further separately divided into an explosive subdomain and a non-explosive subdomain due to the corresponding wall terminations. The three boundaries between the explosive and non-explosive domains yield the three explosion limits.

The relative importance of the wall destruction of the chain carriers in controlling the explosion limits is investigated. The terminations of H and HO_2 are the key steps to break the (R1) and the (R9) chain branching, respectively. It is then demonstrated that the system can retain the Z-shaped explosion limits by keeping only the wall destruction of H and HO_2. In addition, a cubic equation is obtained to describe the Z-shaped explosion limits by further assuming quasi-steadiness of O, OH, and H_2O_2. Based on this equation, the conditions that the explosion limit could lose its Z shape, and thereby possess only a non-explosive regime at lower pressures and an explosive regime at higher pressures, are investigated.

We finally note that this study is restricted to the framework of branched-chain explosions, and that exothermic reactions between the chain carriers may occur near the high-pressure explosion limit. It is then reasonable to anticipate that self-heating could modify the third explosion limit determined herein.[1,15,16] It is nevertheless significant to recognize that system explosion can still occur by accounting for the branched-chain alone, without heat evolvement, as demonstrated herein.

ACKNOWLEDGMENTS

This work was mostly supported by the Center for Combustion Energy at Tsinghua University. The participation of C.K.L. was additionally supported by the Combustion Energy Frontier Research Center, an Energy Frontier Research Center funded by the U.S. Department of Energy, Office of Basic Energy Sciences under Award No. DE-SC0001198.

APPENDIX: A GENERIC MODEL WITH Z-SHAPED EXPLOSION LIMITS

Extending an earlier model for a single branched chain explosion with gas and surface termination reactions,[24] we present in the following a representative scheme incorporating two coupled branched-chains, that illustrates the Z-shaped behavior of an explosive mixture in response to changes in pressure and temperature characteristic of that of the hydrogen-oxygen system.

$nR \xrightarrow{k_I} C$	(R_i)	Chain initiation
$C + R \xrightarrow{k_b} \beta_b C + P$	(R_b)	Low-pressure branching
$C + R + R \xrightarrow{k_g} D + R$	(R_g)	Gas-phase termination of low-pressure branching
$D + R \xrightarrow{k_r} \beta_r C + P$	(R_r)	High-pressure branching
$C \xrightarrow{k_C} P$	(R_C)	Wall destruction of C
$D \xrightarrow{k_D} P$	(R_D)	Wall destruction of D

Here, R is the reactant and P is the stable products formed through the respective reactions. Furthermore, there are two kinds of chain carriers, namely, C and D.

The three-body reaction (R_g) is the gas termination of the low-pressure branched-chain, producing the inactive carrier D, which is subsequently reactivated through (R_r). Thus (R_g) and (R_r) constitute a high-pressure branched-chain, which competes with the low-pressure branching reaction (R_b). The two branched-chains dominate at high and low pressures, respectively.

Here, the rate constants for the gas-phase reactions are $k_b = B_b e^{-T_{a,b}/T}$, $k_g = B_g$, and $k_r = B_r e^{-T_{a,r}/T}$. For the wall destruction of the carriers C and D, the equivalent rate

constants per unit volume are k_C and k_D. Furthermore, the chain branching ratios satisfy β_b, $\beta_r > 1$. To investigate the explosion limits of such a system, we assume constant temperature and reactant concentrations.

For the carriers C and D, the reaction rate equations in matrix form are given as

$$\frac{d}{dt}\begin{pmatrix}[C]\\[D]\end{pmatrix} = A\begin{pmatrix}[C]\\[D]\end{pmatrix} + \begin{pmatrix}I\\0\end{pmatrix}, \tag{A1}$$

where $I = k_I[R]^n$ is the rate of the chain initiation reaction, and the coefficient matrix is

$$A = \begin{bmatrix} A_{11} & A_{12} \\ A_{21} & A_{22} \end{bmatrix}$$

$$= \begin{bmatrix} (\beta_b - 1)k_b[R] - k_g[R]^2 - k_C & \beta_r k_r[R] \\ k_g[R]^2 & -k_r[R] - k_D \end{bmatrix}. \tag{A2}$$

The explosion limits of the system are determined by $\zeta(T, [R]) = 0$, or equivalently $\zeta(T, p/(R^oT)) = 0$ for ideal gases, where ζ denotes the largest real part of the eigenvalues.

The characteristic equation for (A2) is

$$\lambda^2 - (A_{11} + A_{22})\lambda + (A_{11}A_{22} - A_{12}A_{21}) = 0. \tag{A3}$$

Since the discriminant,

$$\Delta = (A_{11} + A_{22})^2 - 4(A_{11}A_{22} - A_{12}A_{21})$$
$$= (A_{11} - A_{22})^2 + 4A_{12}A_{21} > 0,$$

both eigenvalues are real-valued. Therefore, at the explosion limits, their product is zero and their summation is negative, that is,

$$(A_{11}A_{22} - A_{12}A_{21})_{\text{explosion limits}} = 0 \tag{A4}$$

and

$$(A_{11} + A_{22})_{\text{explosion limits}} \le 0. \tag{A5}$$

After some manipulation, from (A4), we obtain the following cubic equation of the reactant concentration, which is proportional to the system pressure, as the neutral condition:

$$(\beta_r - 1)[R]^3 + \left((\beta_b - 1)\frac{k_b}{k_g} - \frac{k_D}{k_r}\right)[R]^2$$
$$+ \left((\beta_b - 1)\frac{k_b}{k_g}\frac{k_D}{k_r} - \frac{k_C}{k_g}\right)[R] - \frac{k_C}{k_g}\frac{k_D}{k_r} = 0, \tag{A6}$$

i.e., $c_3[R]^3 + c_2[R]^2 + c_1[R] + c_0 = 0$. This allows the determination of the critical concentrations at any temperature.

The explosion limits of this model with typical kinetic parameters are shown in Fig. 13.

Noticing the relations $\sqrt{\frac{k_C}{k_g}}$, $\frac{k_b}{k_g} \ll \frac{k_D}{k_r}$, we get the asymptotic explosion limits as follows. At the low-pressure limit, $[R]_{1st} = -\frac{c_0}{c_1} \approx \frac{k_C}{(\beta_b - 1)k_b}$ is obtained from $c_1[R] + c_0 = 0$. Similarly, $[R]_{3rd} = -\frac{c_2}{c_3} \approx \frac{k_D}{(\beta_r - 1)k_r}$ and $[R]_{2nd} = -\frac{c_1}{c_2} \approx \frac{(\beta_b - 1)k_b}{k_g}$ are obtained.

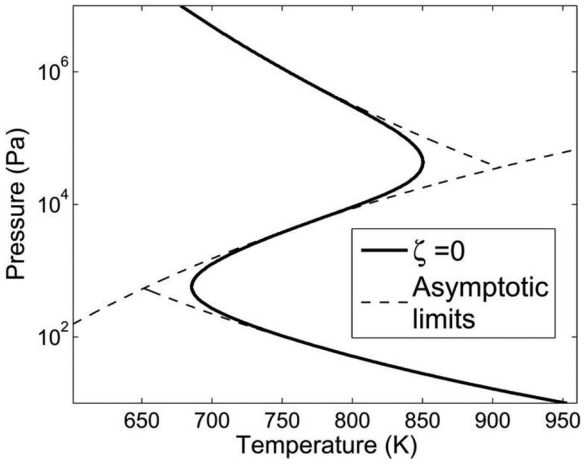

FIG. 13. The Z-shaped explosion limits of the generic model, with the branching ratios $\beta_b = \beta_r = 2$, activation temperatures $T_{ab} = 9000$ K and $T_{ar} = 16\,000$K, preexponential parameters $B_b = B_r = 10^5(\text{mol m}^{-3}\,\text{s}^{-1})$ and $B_g = 1(\text{mol}^2\,\text{m}^{-6}\,\text{s}^{-1})$, and the equivalent volumetric rate constants of the surface terminations $k_C = k_D = 10^{-2}\,\text{s}^{-1}$.

[1] N. N. Semenov, *Some Problems in Chemical Kinetics and Reactivity* (Princeton University, New Jersey, 1959), Vol. 2.
[2] B. Lewis and G. von Elbe, *Combustion, Flames and Explosions of Gases*, 3rd ed. (Academic, New York, 1987).
[3] I. Glassman and R. A. Yetter, *Combustion*, 4th ed. (Elsevier, New York, 2008).
[4] C. K. Law, *Combustion Physics* (Cambridge University, Cambridge, UK, 2006).
[5] R. R. Baldwin and R. F. Simmons, Trans. Faraday Soc. **51**, 680 (1955).
[6] R. R. Baldwin and R. W. Walker, Trans. Faraday Soc. **60**, 1236 (1964).
[7] K. Chinnick, C. Gibson, J. F. Griffiths, and W. Kordylewski, Proc. R. Soc. London, Ser. A **405**, 117 (1986).
[8] K. Chinnick, C. Gibson, and J. F. Griffiths, Proc. R. Soc. London, Ser. A **405**, 129 (1986).
[9] P. Gray, J. F. Griffiths, and S. K. Scott, Proc. R. Soc. London, Ser. A **394**, 243 (1984).
[10] B. F. Gray, Trans. Faraday Soc. **65**, 2133 (1969).
[11] V. V. Voevodsky and R. I. Soloukhin, Sym. (Int.) Combust., [Proc.] **10**, 279 (1965).
[12] J. W. Meyer and A. K. Oppenheim, Sym. (Int.) Combust., [Proc.] **13**, 1153 (1971).
[13] E. S. Oran, T. R. Young, and J. P. Boris, Combust. Flame **48**, 135 (1982).
[14] E. S. Oran and J. P. Boris, Combust. Flame **48**, 149 (1982).
[15] U. Mass and J. Warnatz, Combust. Flame **74**, 53 (1988).
[16] M. Liberman, *Introduction to Physics and Chemistry of Combustion: Explosion, Flame, Detonation* (Springer, Berlin, 2008).
[17] N. N. Semenov, Dokl. Akad. Nauk SSSR **81**, 645 (1951).
[18] A. A. Azatyan, Z. S. Andrianova, and A. N. Ivanova, Kinet. Catal. **51**, 337 (2010).
[19] Z. Hong, D. F. Davidson, and R. K. Hanson, Combust. Flame **158**, 633 (2011).
[20] M. O. Conaire, H. J. Curran, J. M. Simmie, W. J. Pitz, and C. K. Westbrook, Int. J. Chem. Kinet. **36**, 603 (2004).
[21] A. A. Konnov, Combust. Flame **152**, 507 (2008).
[22] M. P. Burke, M. Chaos, Y. Ju, F. L. Dryer, and S. J. Klippenstein, Int. J. Chem. Kinet. **44**, 444 (2012).
[23] R. S. Irving, *Integers, Polynomials, and Rings* (Springer-Verlag, New York, 2004).
[24] R. A. Strehlow, *Fundamentals of Combustion* (McGraw-Hill, New York, 1984).